Transmission Dynamics of and Insights from the 2018-2019 Measles Outbreak in New York City: A Modeling Study

Wan Yang

Department of Epidemiology, Mailman School of Public Health, Columbia University, NY, NY

Correspondence to: wy2202@columbia.edu

Abstract

Background

In 2018-2019, New York City experienced the largest measles outbreak in the US in nearly three decades. The objectives of this study are to identify key population and epidemiological characteristics that may have contributed to this outbreak and gain insights to aid future public health interventions.

Methods and Findings

We developed a model-inference system to infer the transmission dynamics of measles in the affected community and assess the impact of vaccination campaigns implemented during the outbreak, based on monthly age-grouped and overall incidence data reported from Oct 2018 to July 2019. The model-inference system accounted for differential mixing among 5 age-groups (<1, 1-4, 5-17, 18-49, and 50+ years), routine two-dose vaccination, vaccination campaigns, and observational errors including underreporting. However, it did not account for other public health interventions such as post-exposure prophylaxis and school closure.

Approximately 25% of 1-4 year-olds were susceptible when the outbreak began, enabling measles to spread predominantly in this age group in the initial months. Early vaccination campaigns were able to lower this susceptibility and contain measles spread by Dec 2018. However, an increase in infectious contact among 1-4 year-olds, likely facilitated by parents hosting "measles parties" to expose unvaccinated children, appeared to rekindle and aggravate the outbreak in early 2019. Consequently, 1-4 year-olds not only had the largest number of infections (275/642 or 42.8%, as of Aug 6, 2019), but also appeared to cause the largest number of infections in other age groups, including around half of the 100 infections in infants.

The model estimated that, without the implemented vaccination campaigns, there would be 6078 (95% CI: 5, 8433) infections and 452 (95% CI: 0, 628) hospitalizations, including 94 (95% CI: 0, 130) needing intensive care, during the observed outbreak period. In addition, it would largely affect infants under 1 too young to receive the first dose of vaccine and young children under 4, with over 10 times more infections and hospitalizations in both age groups than reported.

Conclusions

These findings highlight the importance of vaccination in protecting children from measles and public health education to reduce activities that unnecessarily expose children to the disease.

Measles is highly contagious and severe viral disease. Thanks to a highly effective vaccine and high coverage of vaccination, endemic transmission of measles—i.e. continuous transmission for more than 12 months—in the US was declared eliminated in 2000. However, due to vaccine hesitancy and declining vaccination rate, in recent years there have been an increasing number of large outbreaks following introduction of measles infection [1]. Due to long-term fluctuations in vaccine coverage and infection history, population susceptibility could vary substantially by age group. This susceptibility disparity by age can further interact with age-specific social connectivity (i.e., contact rate) to shape the epidemic trajectory. As such, understanding these detailed population characteristics as well as their impact on transmission dynamics in the recent outbreaks is important for devising timely and effective intervention strategies.

In the fall of 2018, several New York City (NYC) residents acquired measles while traveling abroad and subsequently led to the largest measles outbreak in the US in nearly three decades. The first case of this outbreak developed a rash on Sep 30, 2018 and as of Aug 6, 2019 (at the time of this writing), there have been 642 confirmed cases, largely occurring in the Orthodox Jewish community [2,3]. To contain the outbreak, the NYC Department of Health and Mental Hygiene (DOHMH) launched extensive vaccination campaigns and, on Apr 9, 2019, ordered mandatary vaccination of all individuals living, working or going to school in the affected zip codes. As a result, over 32 thousand individuals under 19 years were vaccinated with the measles, mumps, and rubella (MMR) vaccine during Oct 2018 – July 2019 and the outbreak subsided [3,4].

66 In this study, we modeled the transmission dynamics of this measles outbreak in the
67 affected Orthodox Jewish community in NYC from Oct 1, 2018 to July 31, 2019, months with
68 more than one measles cases reported. Using an age-structured model-inference framework,
69 we were able to estimate key epidemiological features including the initial susceptibilities in
70 five different age groups (i.e., <1, 1-4, 5-17, 18-49, and 50+ years) and basic reproductive
71 number R_0, infer key factors contributing to the spread of measles, estimate the proportions of
72 infection attributable to each age group, as well as assess the impact of vaccination campaigns.
73

74 **METHODS**

75 The measles outbreak occurred predominantly among members of the Orthodox Jewish
76 community in Williamsburg and Borough Park, two neighborhoods in located in Brooklyn, NYC.
77 As such, we focused on modeling the outbreak in this subpopulation. Estimated based on the
78 Jewish Community Study of New York [5], approximately N=165,970 Orthodox Jews live in
79 these two NYC neighborhoods, of which 4552 (2.7%), 18,208 (11%), 59,176 (35.7%), 60,445
80 (36.4%), and 23,589 (14.2%) are <1, 1-4, 5-17, 18-49, and 50+ years, respectively.
81

82 ***Estimating monthly incidence by age group***

83 Monthly measles incidence aggregated over all ages from Sep 2018 to Aug 2019 and the age
84 distribution of case-patients over the entire outbreak were published on the NYC DOHMH
85 website [3]. Of note, 1 case was reported in Sep 2018 (i.e., the initial case) and none were
86 reported in Aug 2019 at the time of this writing. In addition, the numbers of reported cases
87 were subsequently revised by the DOHMH (often adjusted upwards, presumably from

retrospective case identification) and, as such, varied over time. To estimate the monthly incidence for each age group, we used the age distribution of cases reported in earlier health reports/alerts [6] to apportion the total incidence for each month. For months without age information, we used estimates either from the preceding month or the following month back-calculated from the overall age distribution.

Transmission model

The transmission model used here was similar to described in our previous study [7]. As illustrated in Figure 1, the model represents the susceptible-exposed-infectious-recovered (SEIR) disease dynamics with five age groups (i.e. <1, 1-4, 5-17, 18-49, and 50+ years) to account for population differences by age group (e.g., susceptibility and contact rate), routine two-dose vaccination at ages 1 and 5, and immunization during the vaccination campaigns per Eqn 1:

$$\begin{cases} \frac{dS_i}{dt} = -\left(\frac{S_i^{m_1}}{N_i}\right)\sum_{j=1}^{5}\beta_{ij}\, I_j^{m_2} + k(1-v)N\mathbf{1}_{\boldsymbol{i=1}} + \frac{M}{180}\mathbf{1}_{\boldsymbol{i=1}} + l_{i-1}S_{i-1}(1-v_{i-1}) - l_iS_i - V_i(t) \\ \frac{dE_i}{dt} = \left(\frac{S_i^{m_1}}{N_i}\right)\sum_{j=1}^{5}\beta_{ij}\, I_j^{m_2} - \frac{E_i}{Z} + \alpha_i(t) + l_{i-1}E_{i-1} - l_iE_i \\ \frac{dI_i}{dt} = \frac{E_i}{Z} - \frac{I_i}{D} + l_{i-1}I_{i-1} - l_iI_i \\ \frac{dR_i}{dt} = \frac{I_i}{D} + l_{i-1}R_{i-1} - l_iR_i + l_{i-1}S_{i-1}v_{i-1} + V_i(t) \\ \frac{dM}{dt} = kvN - \frac{M}{180} \end{cases}$$

for i=1,..,5 (Eqn 1)

where S_i, E_i, I_i, R_i and N_i are, respectively, the numbers of susceptible, exposed (i.e. latently infected), infectious, recovered (and/or immunized) people and population size in the i-th age group; M is the number of infants with maternal immunity, which decays exponentially with a

mean duration of 180 days; t is time in days. $V_i(t)$ is the number of people in group-i immunized by the vaccination campaigns on day-t (described in detail in the next section). The exponents m_1 and m_2 describe the level of inhomogeneous mixing [8,9]; and m_1=m_2=1 represents homogeneous mixing. Z and D are the latent and infectious period, respectively.

To model the different contact rates within and between age groups, we used 7 parameters for the Who-Acquires-Infection-From-Whom (WAIFW) matrix as follows:

$$\boldsymbol{\beta} = \begin{bmatrix} \beta_1 & \beta_1 & \beta_1 & \beta_1 & \beta_1 \\ \beta_1 & \beta_2 & \beta_6 & \beta_7 & \beta_1 \\ \beta_1 & \beta_6 & \beta_3 & \beta_7 & \beta_1 \\ \beta_1 & \beta_7 & \beta_7 & \beta_4 & \beta_1 \\ \beta_1 & \beta_1 & \beta_1 & \beta_1 & \beta_5 \end{bmatrix} \quad \text{(Eqn 2)}$$

where β_1 *to* β_5 represent within-group contact for the five age groups and β_6 and β_7 represent mixing between siblings and child-parent, respectively. For simplicity, we set all interactions with group 1 (i.e. <1 year) or group 5 (50+ years) to β_1, the lowest contact rate. For group-3 (5-17 years), to capture the varying contact rate following school schedules, we adjusted β_3 for each date per the school calendar in NYC as:

$$\beta_3(t) = \frac{\beta_3}{b_{Term}} \cdot [1 + b_1 Term(t)] \qquad \text{(Eqn 3)}$$

where b_1 is the amplitude of school term-time forcing; $Term(t)$ is set to 1 for school days and -1 for non-school days; and b_{Term} is the yearly average of $1+b_1 Term(t)$ [10].

The basic reproductive number R_0, defined as the average number of secondary infections caused by a primary case-patient in a *naïve* population, reflects the transmissibility of an infection. In an age-structured model, R_0 is computed as:

$$R_0 = \text{eigen}_{\max}(\boldsymbol{n\beta}D) \qquad \text{(Eqn 4)}$$

where $\text{eigen}_{\max}(\cdot)$ denotes the function giving the largest eigenvalue of a matrix, and $\boldsymbol{n}$ is a diagonal matrix with elements $n_i = N_i/\sum N_i$ (i=1, …, 5 here), i.e. the fraction of population in group-i. Based on this relationship between R_0 and the $\boldsymbol{\beta}$ matrix, we reparametrized the model to include R_0 as a model parameter by setting β_1 to 1 and estimating the relative magnitude of β_2–β_6, all scaled to R_0. In the current mass vaccination era, most people are immune via vaccination. To reflect the potential of an infection to cause an epidemic in a partially susceptible population, the effective reproductive number, R_e, accounts for population susceptibility and is computed as:

$$R_e = \text{eigen}_{\max}(\boldsymbol{s\beta}D) \qquad \text{(Eqn 5)}$$

where $\boldsymbol{s}$ is a diagonal matrix with elements $s_i = S_i/N_i$ (i=1, …, 5 here), i.e. the susceptibility in group-i.

To model the demographic processes, k is the birth rate (2.7 per 1000 person-year here [5]); v is the immunity level in mothers, approximated by the susceptibility of the child-bearing age-group (i.e., 18-49 year-olds); N is total population size; and $\mathbf{1}_{i=1}$ is an indicator function, with value 1 for group-1 (<1 year-olds) and 0 for all other groups. Thus, the term $k(1-v)\,\mathbf{1}_{i=1}$ (1st line in Eqn 1) is the number of susceptible newborns and kvN (last line in Eqn 1) is the number of newborns with maternal immunity. The term l_i is the rate of aging for group-i (i.e. the inverse of the sojourn time in each age group) with l_0 set to 0 and l_5 set to the death rate. The term v_i (for i=1 and 2) is the vaccination rate for the two doses of vaccine (i.e., v_i=0 for i=0, 3, and 4). In this study, we set v_1 (1st dose) to 0.9 times the immunity level of group-2 (i.e., assuming a 90%

147 vaccine efficacy) and v_2 (2nd dose) to 0.7 for days before May 2019; for days afterwards, we
148 used 0.8 for v_1 and 0.9 for v_2, corresponding to a 1-(1-0.8)(1-0.9)=98% overall vaccination rate.
149
150 Based on NYC health reports/alerts [2,11,12], we seeded the model, via the parameter
151 $\alpha_i(t)$, with 3 cases in group-2 (i.e. 1-4 year-olds)—one each with rash onset on Sep 30, Oct 15,
152 and Oct 30, 2018, respectively—and 1 case each in group-3 (5-17 year-olds) and group-4 (18-49
153 year-olds), both during the winter recess (from 12/24/18 to 1/1/19).
154
155 ***Modeling the vaccination campaigns***
156 To contain the outbreak, the NYC DOHMH conducted extensive vaccination campaigns and
157 administered 31,790 doses of MMR vaccine to children under 19 years in Williamsburg and
158 Borough Park by July 2019 [3]. However, information on the age and immune status of
159 vaccinees was not reported. In this study, per the health reports/alters [3,12], we assumed
160 there were two phases of vaccination campaign: 1) Oct 2018 – Feb 2019, during which 7000
161 children, 90% Orthodox Jewish (15% were <1 year, 65% 1-4 years, and 20% 5-17 years) were
162 vaccinated; and 2) Mar – July 2019, during which 24,790 children, 60% Orthodox Jewish (10%,
163 40%, and 50%, respectively, were <1, 1-4, and 5-17 years) were vaccinated. For reference,
164 Orthodox Jews made up for approximately 30% of the total population in the two affected
165 neighborhoods.
166
167 For <1 year-olds, immunization could fail due to residual maternal immunity; thus, we
168 assumed a 85% immunization success rate for group-1. For those above 1 year, some vaccinees

169 might have received 1 or 2 doses of vaccine and higher the population susceptibility, the less
170 likely a vaccinee had been immune before the additional vaccine dose. As such, we assumed
171 the immunization success rate was twice the group-specific susceptibility for 1-4 year-olds and
172 three times that for 5-17 year-olds or at a minimum of 25% and a maximum of 75%. We further
173 assumed a 10-day delay in vaccine effect and computed the daily number of individuals
174 vaccinated per a gamma distribution (mean=30 days and standard deviation=21 days for Phase-
175 1 and mean=56 and standard deviation=15 days for Phase-2 such that it peaked ~1 week after
176 Apr 9, 2019 when the city implemented a vaccination mandate). The estimated numbers
177 matched with the reports (e.g., 1740 doses by our model vs ~1600 doses given to children
178 under 5 as reported [13] and 1142 doses by our model vs ~1000 doses given in March 2019 as
179 reported [14,15]). These daily numbers were then included in the transmission model [i.e. $V_i(t)$
180 in Eqn 1]. Sensitivity to model assumptions were tested as described below.
181
182 ***Estimation of model state variables and parameters***
183 To estimate the model state variables (i.e., S_i, E_i, I_i, R_i, and M) and parameters (β_2 *to* β_7, R_0, b_1, D,
184 Z, m_1, *and* m_2), we fitted the model to the reported monthly overall incidence and the
185 estimated monthly age-grouped incidence using a particle filter [16]. Briefly, we first initialized
186 a suite of model realizations (termed "particles", N=10,000 here) using Latin Hypercube
187 sampling [17] from the prior distribution of state variables and parameters (Table 1). The
188 particle filter then sequentially incorporated the monthly incidence to the model via repeated
189 prediction-update cycles. In each cycle (i.e., each month here), the particles were stochastically
190 integrated forward in time for a month per the model (i.e., Eqn 1; this generates the

prediction). To update the model state including all model variables and parameters, at the end of each month, the model-estimated incidence was aggregated for the month, adjusted by the reporting rate for that month (estimated simultaneously by the filter), and used to compute the likelihood of each particle (described below). The posterior of model state was then computed using Bayes' rule [16,18] and the particles resampled and updated—those with high posterior probabilities were retained and those with very low posterior probabilities discarded.

To allow for a wider observational variance than, e.g., the Poisson process, we heuristically modeled the observations using a multivariate Gaussian distribution (i.e. the likelihood function):

$$\boldsymbol{Y_m} | r, \boldsymbol{C_m} \sim \mathcal{N}(r\boldsymbol{C_m}, \boldsymbol{\Sigma}) \quad \text{(Eqn 6)}$$

where $\boldsymbol{Y_m}$ is the vector of monthly incidence reported for month-*m*, including the monthly incidence for individual age-groups (i.e., <1, 1-4, 5-17 and 18+ years; note that 18-49 and 50+ year-olds were combined due to a lack of data for these two groups separately) and all ages combined. Correspondingly, $\boldsymbol{C_m}$ is the vector of monthly incidence estimated by the model; and *r* is the reporting rate and, for simplicity, assumed the same for all ages. $\boldsymbol{\Sigma}$ is the covariance matrix, with the off-diagonal terms set to 0. To account for uncertainties in the estimated age-grouped incidence, the variance ($\Sigma_{ii}, i = 1, \ldots, 4$) for each of the 4 aforementioned age-groups was heuristically computed as:

$$\Sigma_{ii,m} = 100 + \frac{\left(\sum_{m}^{m-2} Y_m/3\right)^2}{3} \quad \text{(Eqn 7a)}$$

212 That is, the observational variance is proportional to the average incidence in the preceding
213 two months (if available) and the current month, plus a baseline constant. For the overall
214 incidence with detailed data, a smaller variance was used:

215 $$\Sigma_{ii,m} = 100 + \frac{\left(\sum_{m}^{m-2} Y_m/3\right)^2}{5} \text{ (Eqn 7b)}$$

216

217 As there were great uncertainties in the susceptibilities of the younger age groups, we
218 tested prior ranges from 10-40% for 1-4 year-olds, 5-20% for 5-17 year-olds, and 5-15% for 18-
219 49 year-olds. For the basic reproductive number R_0, we tested prior values ranging from 5 to 12
220 (note these values were lower than the oft-reported 12-18 range [19,20]). To optimize the
221 model-filter system, we parsed these wide ranges into smaller segments and tested all
222 combinations by permutation (5040 in total; see specific prior ranges in Table 1). To account for
223 model stochasticity, we ran the model-filter system 5 times for each prior combination and 10
224 times for the final prior select. We then selected the optimal priors based on the model-
225 goodness-of-fit to the data (minimal root-mean-square-error and maximal correlation and
226 likelihood) over the period of Oct 2018 – July 2019 as well as accuracy of the one-step-ahead
227 predictions (recall that the particle filtering process comprises sequential prediction-update
228 cycles) for the period of Oct 2018 – March 2019 (i.e. before the emergency vaccination
229 mandate). We pooled all 10 final runs (10,000 particles each run and 100,000 model
230 realizations in total) to compute the posterior estimates [e.g., mean and 95% credible intervals
231 (CI)].

232

233 ***Sensitivity analysis on vaccination campaigns settings***

234 To test the sensitivity of model results to assumptions on vaccination campaign settings, we
235 tested the model-filter system using the following alternative scenarios:
236 1) For the 2nd phase (Mar-July 2019), 90% (vs. 60% in the baseline scenario) of the
237 vaccine doses were given to members of the Orthodox Jewish community;
238 2) For the 2nd phase, the age distribution of vaccinees was the same as the 1st phase (i.e.
239 15%, 65%, and 20%, respectively, for <1, 1-4, and 5-17 year-olds vs. 10%, 40%, and 50% for the
240 three groups in the baseline scenario);
241 3) For the 2nd phase, 90% of the vaccine doses were given to Orthodox Jewish and the
242 age distribution of vaccinees was the same as the 1st phase (i.e. 15%, 65%, and 20% for <1, 1-4,
243 and 5-17 year-olds, respectively).
244
245 Because population susceptibility would be affected by the number of individuals
246 immunized by the vaccination campaigns, we tested susceptibility ranges 10-40% for 1-4 year-
247 olds, 5-20% for 5-17 year-olds, and 5-15% for 18-49 year-olds, divided in to small segments as
248 for the baseline scenario (140 different combinations for each alternative scenario; Table 1).
249 For simplicity, we used the same optimal prior ranges for the parameters under the baseline
250 scenario in this sensitivity analysis.
251
252 ***Evaluating the impact of vaccination campaigns***
253 To estimate the impact of vaccination campaigns, we generated model-simulated
254 counterfactuals—i.e., outbreak outcomes should there be no vaccination campaigns
255 implemented—using the posterior mean estimates of group-specific initial population

susceptibilities and model parameters for each month. We ran the model (10,000 realizations) stochastically up to the end of 2019 to test how long the outbreak could last without intervention; for months after Aug 2019, parameters estimated at the end of July 2019 were used.

RESTULTS

Overview of the measles outbreak and model fit

The measles outbreak started on Sep 30, 2018, when a young child developed a rash. It evolved relatively slowly in the first three months; however, the outbreak took off quickly in early 2019, peaked in April after the city declaring a public health emergence, and recorded a total of 642 cases by July 31, 2019. As shown in Figure 2, age-grouped incidence, estimated based on health reports/alerts [3,6], peaked first in Mar 2019 among 1-4 year-olds—the age group with the largest number of infection (275 cases or 42.8% of the total, as of Aug 6, 2018), followed by <1 year-olds (100 cases or 15.6%) and 5-17 year-olds (138 cases or 21.5%) in Apr 2019, and 18+ year-olds (129 cases or 20.1%) in May 2019.

The model-filter system was able to recreate the overall incidence curve during Oct 2018 – July 2019, estimate the overall age distribution of measles cases, as well as recreate the estimated age-grouped incidence curves for all age groups (Figure 3 and Table S1). Note that while our model (Eqn 1) divided 18+ year-olds into two subgroups (i.e. 18-49 and 50+ years) given their differences in contact rates and interactions with other age-groups, we present the combined results here because data were only available for the entire age group. The

278 estimated reporting rate was around 90% throughout the study period and slightly lower in Apr
279 2019, at the peak of the outbreak (89.1%, 95% CI: 79.4, 99.2%; Figure S1).
280
281 ***Inference of key epidemiological characteristics***
282 The model-filter system estimated that, at the beginning of the outbreak (i.e. Sep 2018),
283 susceptibility was the highest in infants, at approximately 53.2% (95% CI: 49.0, 57.5%; Figure
284 4A). This was expected, because maternal immunity wanes within 3 to 9 months after birth
285 and, as a result, by their first birthday—the age eligible to receive the first dose of MMR vaccine
286 in the US—almost all infants have lost their maternal immunity and are susceptible to measles.
287 Young children aged 1-4 years had the second highest susceptibility; approximately 24.9% (95%
288 CI: 20.4, 29.7%) were susceptible. In comparison, susceptibility was lower among both 5-17
289 year-olds (6.0%, 95% CI: 4.1, 7.9%) and 18+ year-olds 6.0% (95% CI: 4.4, 7.6%; Figure 4). These
290 estimates were consistent with the observation that all cases recorded in Oct 2018 were
291 children ranging from 11 months to 4 years [2]. Sensitivity analysis on assumptions related to
292 the vaccination campaigns showed that estimated susceptibilities were slightly higher for 5-18
293 year-olds (7.5%, 95% CI: 5.1, 9.9%) and 18-49 year-olds (7.9%, 95% CI: 5.2, 9.9%) if more vaccine
294 doses were given to the Jewish Orthodox community or 5-18 year-olds; however, the estimates
295 were in general consistent with the baseline scenario (Table S1).
296
297 The initial vaccination campaigns launched promptly afterwards lowered the
298 susceptibility to 40.3% (95% CI: 36.4, 44.0%) in infants and 13.9% (95%: 9.7, 18.7%) in 1-4 year-
299 olds, by the end of Dec 2018 (Figure 4). These efforts along with other transmission and

300 infection controls [2] appeared to effectively contain the outbreak at the time. The effective
301 reproductive number (R_e) is a key epidemiological parameter reflecting the potential of an
302 infection to cause an epidemic in a partially immune population; an epidemic is possible when
303 R_e>1. The estimated R_e was 1.5 (95% CI: 0.7, 2.9) in Oct 2018 and dropped to round 1 (95% CI:
304 0.7, 1.5) in Dec 2018 (Figure 5B).
305
306 The outbreak, however, took off again in early 2019 (Figure 2). The estimated R_e
307 increased and remained above 1 in the first three months of 2019 (Figure 5B). In a perfectly
308 mixed model, R_e is computed as the product of the basic reproductive number R_0 and
309 population susceptibility. In particular, the basic reproductive number R_0 measures the
310 transmissibility of an infection in a fully susceptible population; for measles, while often
311 reported in the range of 12-18, R_0 could vary from 1.4 to 770 [19]. In this study, we estimated
312 that R_0 was approximately 7 during the entire outbreak (Figure 5A). Population susceptibility,
313 the other factor for R_e, were to increase in a close population (i.e., without migration), could
314 only do so slowly as infants lose maternal immunity. Thus, these two factors alone could not
315 explain the sudden large increase in R_e (Figure 5B). In this study, we utilized an age-structured
316 model that enables more detailed analysis of the transmission dynamics. Indeed, our model-
317 filter system detected an increase in contact rate among 1-4 year-olds during Jan-March 2019
318 (Figure 5D); this increased contact rate along with the high susceptibility among 1-4 year-olds
319 appeared to raise R_e above unity (Eqn 5) and contribute to the re-surge of measles in early
320 2019. This finding was also consistent with reports of parents hosting "measles parties" to
321 exposure unvaccinated children at the time [14]. In contrast, estimated contact rates were

322 relatively stable for other age groups (e.g., Figure 5 E and F for 5-17 and 18-49 year-olds,
323 respectively). As a result, infections increased quickly among 1-4 year-olds (Figures 2 and 5D),
324 reaching a peak of around 80 cases in March. Meanwhile, infections also increased in other age
325 groups including 5-17 and 18+ year-olds despite their low overall susceptibilities, due to
326 interactions between age-groups (Figure S1) and the high contact rates in these groups (Figure
327 5 E and F).
328
329 The outbreak began to decline in Apr 2019, following more stringent public health
330 interventions [3,4]. In particular, the model estimated that, thanks to extensive vaccination
331 campaigns, susceptibility was reduced to 22.8% (95% CI: 19.3, 26.0%) in <1 year-olds, 4.3%
332 (95% CI: 0.5, 8.9%) in 1-4 year-olds, and 2.4% (95% CI: 0.4, 4.4%) in 5-17 year-olds at the end of
333 May. Consequently, the effective reproductive number R_e dropped below 1 from April onwards.
334
335 ***Who acquired infection from whom?***
336 Table 2 shows the estimated proportions of infections caused by each of the five age groups
337 based on the estimated WAIFW contact matrix (Eqn 2). Children aged 1-4 years not only had
338 the largest number of infections (42.8%), but also appeared to cause the largest number of
339 infections in other age groups. Tallied over the entire study period (Oct 2018-July 2019), an
340 estimated 51.6% (95% CI: 39.3, 63.1%) of the total cases were infected by 1-4 year-olds,
341 compared to 25.2% (95% CI: 15.8, 35.5%) by 5-17 year-olds, 17.7% (95% CI: 10.4, 26.5%) by 18-
342 49 year-olds, 4.5% (95% CI: 3.0, 6.4%) by <1 year-olds, and 1.0% (95% CI: 0.4, 1.8%) by 50+ year-
343 olds. In particular, this age group caused around half of the infections in infants (44.6% or 45

344 cases) as well as the largest proportions of inter-group transmission to other age-groups
345 (ranging from 12.9% to 5-17 year-olds to 40.1% to 50+ year-olds; Table 2).
346
347 ***Estimated impact of vaccination campaigns***
348 Figure 6 shows the estimated outbreak outcomes had there be no vaccination campaigns.
349 Without the vaccination campaigns, the model estimated that the outbreak could continue to
350 the end of 2019 and infect a total of 6196 (95% CI: 5, 8478) people by then or 6078 (95% CI: 5,
351 8433) during the observed outbreak period (i.e. Oct 2018 – July 2019), compared to 642 cases
352 reported as of Aug 6, 2019. In addition, these infections would largely occur in infants under 1
353 and young children aged 1-4 years. During the observed outbreak period, there would be 1015
354 (95%: 0, 1430) infections in infants and 3052 (95% CI: 2, 4096) infections in 1-4 year-olds, more
355 than 10 times of the reported numbers in these two age groups (i.e. 100 and 275, respectively,
356 as of Aug 6, 2019; Table 3). Children aged 5-17 years would have the third largest number of
357 infections, with 1107 (95% CI: 1, 1692) cases, 8 times of the reported number (i.e. 138 as of Aug
358 6, 2019).
359
360 Measles can cause severe diseases. According to data by Apr 24, 2019, among 390
361 individuals with measles, 29 were hospitalized, of which six needed intensive care [21].
362 Assuming the same ratios among all cases, without the vaccination campaigns, during the
363 observed outbreak period there would be 452 (95% CI: 0, 628) hospitalizations, including 94
364 (95% CI: 0, 130) needing intensive care, and the majority would be in young children under 4
365 (Table 3).

366

367 **DISUCSSION**

368 Using a model-filter inference system, we have reconstructed in detail the transmission
369 dynamics of the measles outbreak in an Orthodox Jewish community in NYC during Oct 2018 –
370 July 2019. We have estimated the population characteristics (e.g. age-specific susceptibilities)
371 and epidemiological parameters (e.g. reproductive numbers) as well as subtle changes in key
372 parameters (e.g. contact rates) that are critical to the transmission of measles. Using model
373 simulation and the posterior estimates from the model-inference system, we are also able to
374 estimate the impact of vaccination campaigns implemented during the outbreak, including
375 numbers of infections and hospitalizations averted, for each age group. These latter findings
376 echo those from previous studies [22-24] and again highlight the severity of measles disease,
377 should there be no effective infection and transmission controls (in particular, vaccination).

378

379 Our analyses estimate that around a quarter of young children aged 1-4 in the affected
380 community were susceptible at the onset of the outbreak, likely due to delayed vaccination.
381 Indeed, 94% (101/108) of the early infections in children were unvaccinated [12]. In contrast,
382 vaccination rate remained high in older children 5-17 years, with an estimated 94% immune to
383 measles. This difference may be due to better compliance with vaccination regulation at school
384 entry, or a result of vaccination campaigns in response to previous outbreaks (e.g., a large
385 outbreak occurred in the same community in 2013 [25]). Nevertheless, the large number of
386 unvaccinated children under 4 was sufficient to cause many infections in late 2018,
387 predominantly in the same age group (Figure 2 and references [2,11,12]). This observation

388 highlights the importance of vaccination compliance with both MMR vaccine doses, especially
389 given the long lag between the two vaccine doses.
390
391 Our study also reveals intricate interplays of population dynamics and measles
392 transmission. While the high susceptibility in children under 4 was likely responsible for the
393 early spread of measles, our estimates suggest that the second and more severe part of the
394 outbreak in 2019 was likely due to increased infectious contact among this age group, likely
395 facilitated by parents hosting "measles parties" that intentionally bring unvaccinated children
396 together and expose them to those sick with measles [14]. As shown in Figure 5, the increase in
397 infectious contact interacting with the high susceptibility in 1-4 year-olds was able to raise the
398 effective reproductive number R_e to above unity—the threshold for an epidemic to occur—and
399 aggravate the outbreak in 2019, despite earlier public health efforts that had reduced R_e to
400 below 1 in late 2018. Similar disease-related gatherings have been noted in previous measles
401 outbreaks [26] as well as other disease outbreaks [27]. These activities create further
402 challenges for the control of measles spread and stress the need for enhanced public health
403 education.
404
405 In addition, the intensified measles outbreak not only affected children with delayed
406 vaccination, but also a large number of infants under 1, who were too young to receive their
407 first dose of MMR vaccine in the US. At least 100 infants under 1 were infected with measles
408 during the 10-month outbreak period, despite extensive infection and transmission control
409 efforts including vaccinating infants 6 months or older and post-exposure prophylaxis with

410 immune globulin given to those under 6 months [2,11]. This was largely a result of the high
411 susceptibility in infants. Our model-inference system estimates that about half of infants were
412 susceptible by age 1 and that nearly half of the 100 infant cases were infected by 1-4 year-olds
413 (Table 2). In addition, our simulations suggest that, without the vaccination campaigns, the
414 number of infections in infants would be over 10 times higher than observed (Table 3). These
415 findings demonstrate the rippling effects of vaccine hesitancy beyond the risk posted to age-
416 eligible children with delayed vaccination. These findings also suggest that administration of
417 the first dose of routine MMR vaccine earlier than the current 1 year age-limit in the US may be
418 necessary to protect infants should the high level of vaccine hesitancy persist.
419
420 Our model simulations, consistent with many previous studies [24,26,28], demonstrate
421 the significant public health impact of vaccination in controlling measles outbreaks. Without the
422 implemented vaccination campaigns, the severity of the measles outbreak—including number
423 of infections, hospitalizations, and severe infections needing intensive care—would be about 10
424 times worse than observed (Table 3). These estimates, however, did not include the long-term
425 health impacts on affected individuals, particularly young children [23,29], nor the enormous
426 economic burdens [25,30,31].
427
428 We note several limitations of our study. First, we did not explicitly model the impact
429 of public health interventions other than the vaccination campaigns, due to a lack of data.
430 During the outbreak, such efforts included prescreening patients prior to presence for
431 treatment, post-exposure prophylaxis, and closing schools out of vaccination compliance

432 [2,11,12,32,33]. Of note, however, here the estimated basic reproductive number R_0 was
433 around 7, lower than the 12-18 range based on epidemics in the pre-vaccine era [20]; and the
434 estimated infectious period was around 4 days (Figure 5C), at the lower end of the commonly
435 used range of 4-6 days [34]. The lower R_0 and shorter infectious period could be a result of the
436 aforementioned public health interventions. Second, there were uncertainties in the accuracy
437 of case reporting. Because the incidence data used here were published on Aug 6, 2016, a later
438 revision of case reports, we used a relatively high but broad prior range for the reporting rate
439 (i.e. 80-100%). In addition, our model-inference system explicitly accounted for observational
440 errors (Eqn 7a and 7b). Third, due to a lack of contact data and for simplicity, we set all terms
441 related to group-1 (i.e. <1 year-olds) in the WAIFW matrix to the same as the contact rate
442 within the group (Eqn 2). The model formulation may have led to under-estimation of the
443 proportions of infection in <1 year-olds attributable to the same age group and/or 1-4 year-
444 olds, given the likely more frequent contact within the same age group and with similar ages
445 (i.e. 1-4 years) due to more shared settings such as daycares and pediatric hospitals. Lastly,
446 there were uncertainties regarding the settings of vaccination campaigns. Nevertheless,
447 sensitivity analysis showed that our main estimates were robust to a wide range of assumptions
448 (Table S1).
449
450 In summary, using a comprehensive model-inference system, we have reconstructed
451 transmission dynamics of the recent measles outbreak in NYC in great detail. Our estimates
452 highlight the importance of vaccination in protecting children as well as public health education
453 to reduce activities that unnecessarily expose children to risk of measles infection.

Acknowledgements

I thank all public health personnel and individuals involved in combating the measles outbreak and New York City Department of Health and Mental Hygiene for making the incidence data publicly available. I also thank Columbia University Mailman School of Public Health for access to high performance computing.

Finding source: This study was supported by the National Institute of Allergy and Infectious Diseases (1R01AI145883-01).

Conflict of interest: None.

References:

1. Phadke VK, Bednarczyk RA, Salmon DA, Omer SB (2016) Association between vaccine refusal and vaccine-preventable diseases in the United States a review of measles and pertussis. Jama-J Am Med Assoc 315: 1149-1158.
2. New York City Department of Health and Mental Hygiene. (2018) Alert # 39: Update on measles outbreak in New York City in the Orthodox Jewish community. https://www1.nyc.gov/assets/doh/downloads/pdf/han/alert/2018/alert39-measles-outbreak.pdf
3. New York City Department of Health and Mental Hygiene. (2019) Measles. https://www1.nyc.gov/site/doh/health/health-topics/measles.page
4. New York City Department of Health and Mental Hygiene. (2019) Order of the commissioner. https://www1.nyc.gov/assets/doh/downloads/pdf/press/2019/emergency-orders-measles.pdf
5. Beck P, Cohen SM, Ukeles JB, Miller R (2013) Jewish community study of New York: 2011, geographic profile. Revised ed. New York City: UJA-Federation of New York.
6. New York City Department of Health and Mental Hygiene. (2019) Health alert network. https://www1.nyc.gov/site/doh/providers/resources/health-alert-network.page
7. Yang W, Li J, Shaman J (2019) Characteristics of measles epidemics in China (1951-2004) and implications for elimination: A case study of three key locations. Plos Comput Biol 15: e1006806.
8. Finkenstädt BF, Grenfell BT (2000) Time series modelling of childhood diseases: A dynamical systems approach. Journal of the Royal Statistical Society: Series C (Applied Statistics) 49: 187-205.

9. Liu W-M, Hethcote HW, Levin SA (1987) Dynamical behavior of epidemiological models with nonlinear incidence rates. Journal of mathematical biology 25: 359-380.
10. Keeling MJ, Rohani P (2008) Temporally forced models. Modeling infectious diseases in humans and animals. 1st ed: Princeton University Press. pp. 155.
11. New York City Department of Health and Mental Hygiene. (2018) Alert # 38: Measles outbreak in New York City in the Orthodox Jewish community. https://www1.nyc.gov/assets/doh/downloads/pdf/han/alert/2018/alert38-measles-outbreak.pdf
12. New York City Department of Health and Mental Hygiene. (2019) Alert # 2: Update on measles outbreak in New York City in the Orthodox Jewish community. https://www1.nyc.gov/assets/doh/downloads/pdf/han/alert/2019/update-on-measles-outbreak-in-nyc-in-the-orthodox-jewish-community.pdf
13. New York City Department of Health and Mental Hygiene. (2018) Health department reports eleven new cases of measles in brooklyn's Orthodox Jewish community, urges on time vaccination for all children, especially before traveling to israel and other countries experiencing measles outbreaks. https://www1.nyc.gov/site/doh/about/press/pr2018/pr091-18.page
14. Scutti S. (2019) New York City declares a public health emergency amid Brooklyn measles outbreak. https://www.cnn.com/2019/04/09/health/measles-new-york-emergency-bn/index.html
15. New York City Department of Health and Mental Hygiene. (2019) Measles outbreak in Orthodox Jewish community of Brooklyn continues to grow — health department urges parents to vaccinate their children. https://www1.nyc.gov/site/doh/about/press/pr2019/measles-outbreak-now-at-121-cases.page
16. Arulampalam MS, Maskell S, Gordon N, Clapp T (2002) A tutorial on particle filters for online nonlinear/non-Gaussian Bayesian tracking. IEEE Trans Signal Process 50: 174-188.
17. Mckay MD, Beckman RJ, Conover WJ (1979) Comparison of three methods for selecting values of input variables in the analysis of output from a computer code. Technometrics 21: 239-245.
18. Yang W, Karspeck A, Shaman J (2014) Comparison of filtering methods for the modeling and retrospective forecasting of influenza epidemics. PLoS Comput Biol 10: e1003583.
19. Guerra FM, Bolotin S, Lim G, Heffernan J, Deeks SL, et al. (2017) The basic reproduction number (R0) of measles: A systematic review. Lancet Infect Dis 17: e420-e428.
20. Anderson RM, May RM (1991) Infectious diseases of humans: Dynamics and control. Oxford: Oxford University Press.
21. New York City Department of Health and Mental Hygiene. (2019) Alert # 9: Citywide recommendations during the ongoing measles outbreak in New York City. https://www1.nyc.gov/assets/doh/downloads/pdf/han/alert/2019/recommendations-during-measles-outbreak.pdf
22. Mina MJ, Grenfell BT, Metcalf CJE (2019) Response to comment on "long-term measles-induced immunomodulation increases overall childhood infectious disease mortality". Science 365.

530 23. Mina MJ, Metcalf CJE, De Swart RL, Osterhaus ADME, Grenfell BT (2015) Long-term
531 measles-induced immunomodulation increases overall childhood infectious disease
532 mortality. Science 348: 694-699.
533 24. Gastanaduy PA, Funk S, Paul P, Tatham L, Fisher N, et al. (2018) Impact of public health
534 responses during a measles outbreak in an Amish community in Ohio: Modeling the
535 dynamics of transmission. Am J Epidemiol 187: 2002-2010.
536 25. Rosen JB, Arciuolo RJ, Khawja AM, Fu J, Giancotti FR, et al. (2018) Public health
537 consequences of a 2013 measles outbreak in New York City. JAMA Pediatr 172: 811-817.
538 26. Gastanaduy PA, Banerjee E, Debolt C, Bravo-Alcantara P, Samad SA, et al. (2018) Public
539 health responses during measles outbreaks in elimination settings: Strategies and
540 challenges. Human vaccines & immunotherapeutics 14: 2222-2238.
541 27. Centers for Disease Control and Prevention. (2018) Chickenpox (varicella): Transmssion.
542 https://www.cdc.gov/chickenpox/about/transmission.html
543 28. Lessler J, Metcalf CJE, Cutts FT, Grenfell BT (2016) Impact on epidemic measles of
544 vaccination campaigns triggered by disease outbreaks or serosurveys: A modeling study.
545 Plos Medicine 13.
546 29. Christensen PE, Schmidt H (1953) An epidemic of measles in southern greenland 1951;
547 measles in virgin soil. Iv. The significance of specific prophylaxis. Acta Med Scand 145:
548 126-142.
549 30. Chen SY, Anderson S, Kutty PK, Lugo F, Mcdonald M, et al. (2011) Health care-associated
550 measles outbreak in the United States after an importation: Challenges and economic
551 impact. Journal of Infectious Diseases 203: 1517-1525.
552 31. Dayan GH, Ortega-Sanchez IR, Lebaron CW, Quinlisk MP, Team IMR (2005) The cost of
553 containing one case of measles: The economic impact on the public health
554 infrastructure - iowa, 2004. Pediatrics 116: E1-E4.
555 32. Pager T. (2019) Measles outbreak: Yeshiva's preschool program is closed by New York City
556 health officials. https://www.nytimes.com/2019/04/15/nyregion/measles-nyc-yeshiva-
557 closing.html
558 33. Sanders A. (2019) NYC health officials close two more Williamsburg yeshivas for failure to
559 show immunization records amid measles outbreak.
560 https://www.nydailynews.com/news/politics/ny-city-closes-williamsburg-brooklyn-
561 yeshivas-measles-outbreak-20190613-jogozcbe65ejtalweq255lwkka-story.html
562 34. Keeling MJ, Grenfell BT (1997) Disease extinction and community size: Modeling the
563 persistence of measles. Science 275: 65-67.
564

TABLES

Table 1. Main model parameters and prior ranges tested. In total, we tested 5040 combinations of prior ranges. Each combination was used as the lower and upper bounds of Latin Hypercube sampling. The optimal prior used in the final model-filter runs are bolded if multiple ranges were tested.

Parameter	Symbol/Equation	Ranges tested
Initial susceptibility in <1 year-olds	S_1(t=0); Eqn 1	Based on susceptibility in 18-49 year-olds (i.e., the mothers)
Initial susceptibility in 1-4 year-olds	S_2(t=0); Eqn 1	[5, 15], [10, 20], [15, 25], **[20, 30]**, [25, 35], [30, 40], [35, 45]%
Initial susceptibility in 5-17 year-olds	S_3(t=0); Eqn 1	**[4, 8]**, [5, 10], [5, 15], [10, 20], [15, 25]%
Initial susceptibility in 18-49 year-olds	S_4(t=0); Eqn 1	**[4, 8]**, [5, 10], [5, 15], [10, 20]%
Initial susceptibility in 50+ year-olds	S_5(t=0); Eqn 1	[4, 8]%
Initial number of infants with maternal immunity	M(t=0); Eqn 1	Based on susceptibility in 18-49 year-olds (i.e., the mothers)
Latent period	Z; Eqn 1	[7, 9] days
Infectious period	D; Eqn 1	[2, 6] days
Mixing parameter for the susceptibles	m_1; Eqn 1	**1** (perfect mixing), [0.95, 1], [0.9, 0.95]
Mixing parameter for the infectious	m_2; Eqn 1	**1** (perfect mixing), [0.95, 1], [0.9, 0.95]
Relative contact rate among <1 year-olds	β_1; Eqn 2	Set to 1
Relative contact rate among 1-4 year-olds	β_2; Eqn 2	[3, 30]
Relative contact rate among 5-17 year-olds	β_3; Eqn 2	[25, 50]
Relative contact rate among 18-49 year-olds	β_4; Eqn 2	[20, 40]
Relative contact rate among 50+ year-olds	β_5; Eqn 2	[1, 5]
Relative contact rate between 1-4 and 5-17 year-olds (sibling interactions)	β_6; Eqn 2	[1, 5]
Contact rate between 18-49 and 1-4 or 5-17 year-olds (parent-child interactions)	β_7; Eqn 2	[1, 5]
Amplitude of school term-time forcing	b_1; Eqn 3	[0.25, 0.75], **[0.5, 1]**
Basic reproductive number	R_0; Eqn 4	**[5, 10]**, [7, 12]
Reporting rate	r; Eqn 6	[80, 100]%

Table 2. Estimated proportion of infections caused by each age-group. Rows show the receiving (i.e. infectee) age groups and columns show the source of infection (i.e. infector age group). The numbers are the mean (and 95% CI) estimates in percentage. For instance, for <1 year-olds (3rd row), on average 16.3% of cases were infected by the same age group, 44.6% by 1-4 year-olds, 20.9% by 5-17 year-olds, 15.2% by 18-49 year-olds, and 3% by 50+ year-olds.

Infectee age groups	Infector age groups				
	<1 year	1-4 years	5-17 years	18-49 years	50+ years
<1 year	16.3 (12.3, 21.0)	44.6 (35.5, 53.5)	20.9 (13.9, 28.4)	15.2 (9.6, 21.6)	3.0 (1.4, 5.0)
1-4 years	1.8 (1.0, 3.0)	85.8 (77.0, 91.9)	7 (3.2, 12.9)	5 (2.2, 9.3)	0.3 (0.1, 0.6)
5-17 years	1.5 (0.9, 2.4)	12.9 (6.9, 21.3)	80.9 (70.4, 88.4)	4.4 (2, 8)	0.3 (0.1, 0.5)
18-49 yeas	2.4 (1.5, 3.7)	18.6 (10.9, 28.0)	9.1 (4.8, 14.9)	69.5 (56.2, 80.8)	0.4 (0.2, 0.8)
50+ years	15.5 (11.6, 19.9)	40.1 (31.1, 49.3)	19.7 (13, 27)	15.6 (9.7, 22.4)	9.1 (3.8, 16.3)

Table 3. Estimated impact of vaccination campaigns during Oct 2018 – July 2019. Columns 2-4 show the total numbers of infections (2nd column), hospitalizations (3rd column), and individuals in intensive care unit (ICU) for different age groups (rows 3 to 6) and overall (last row), should there be no vaccination campaigns. Columns 5-7 show the number of infections, hospitalizations, and ICU cases averted by the vaccination campaigns, compared to data reported as of Aug 6, 2019. Numbers are the mean (and 95% confidence intervals) of 10,000 simulations.

Age group	No. if without vaccination campaigns			No. averted by vaccination campaigns		
	Infection	Hospitalization	ICU	Infections	Hospitalization	ICU
<1	1015 (0, 1430)	75 (0, 106)	16 (0, 22)	937 (0, 1330)	70 (0, 99)	14 (0, 20)
4-5	3052 (3, 4096)	227 (0, 305)	47 (0, 63)	2837 (0, 3821)	211 (0, 284)	44 (0, 59)
5-17	1107 (1, 1692)	82 (0, 126)	17 (0, 26)	999 (0, 1554)	74 (0, 116)	15 (0, 24)
18+	904 (1, 1343)	67 (0, 100)	14 (0, 21)	803 (0, 1214)	60 (0, 90)	12 (0, 19)
All	6078 (5, 8443)	452 (0, 628)	94 (0, 130)	5576 (0, 7801)	415 (0, 580)	86 (0, 120)

FIGURES

Figure 1. Schematic of the measles transmission model. Measles transmission model follows the susceptible (S), exposed (E) and latently infected, infectious (I), and recovered (R) and/or immunized SEIR dynamics and includes 5 age-groups as indicated by the subscripts (i.e., <1, 1-4, 5-17, 18-49, and 50+ year-olds, respectively) and a group (M) for infants with maternal immunity. Black solid arrows show the disease-related processes; grey solid arrows show the demographic processes including birth (horizontal), aging (vertical), and death (tilted). Black dashed arrows show processes related to the routine 2-dose measles vaccination where susceptible individuals are vaccinated at ages 1 and 5 and move to the respective immune groups. Red dotted arrows show processes related to vaccination of susceptible individuals under 18 during the vaccination campaigns.

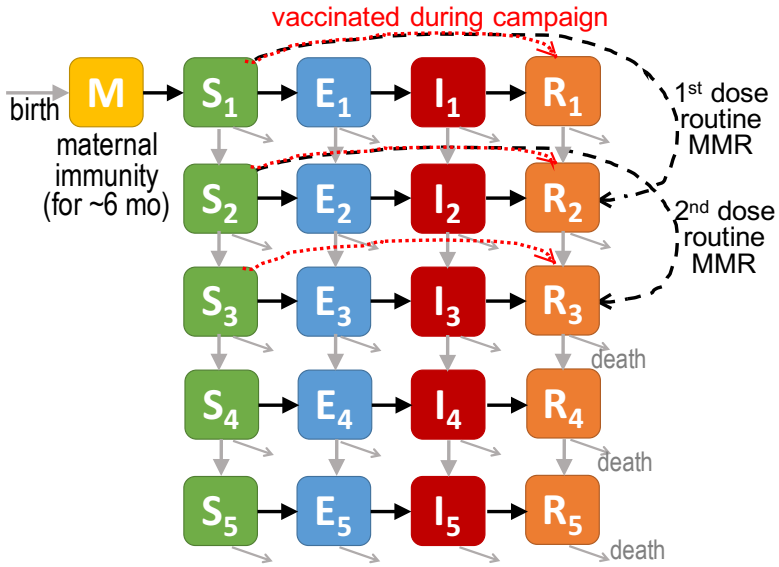

Figure 2. Monthly incidence for all ages and by age group. The solid line (y-axis on the right) shows monthly incidence for all ages, reported as of Aug 6, 2019. For comparison, bars (y-axis on the left) show monthly incidence for <1 (blue), 1-4 (orange), 5-17 (grey) and 18+ (yellow) year-olds, respectively, estimated based on health reports.

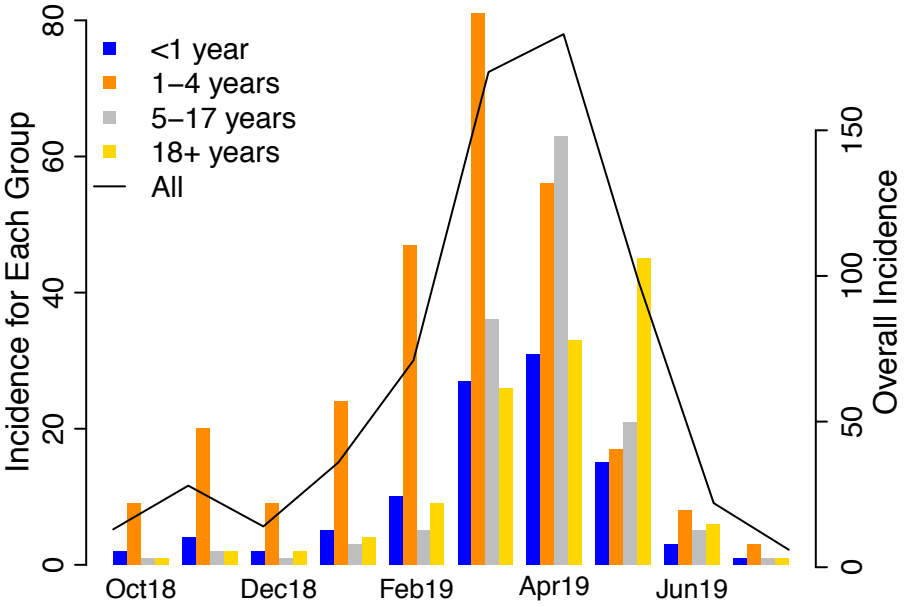

Figure 3. Model fit. Box plots show estimates of monthly incidence for all ages (A), percentage of cases reported in each age group (B), and monthly incidence for <1 year-olds (C), 1-4 year-olds (D), 5-17 year-olds (E), and 18+ year-olds (F). Results are pooled over all 10 model-filter runs (each with 10,000 and in total 100,000 model realizations). Horizontal thick lines show the median of model estimates; box edges show the 25th and 75th percentiles; whiskers show the 2.5th and 97.5th percentiles; and dots show outliers. Stars (*) in A and B show monthly incidence for all ages and the age distribution, reported as of Aug 6, 2019; crosses (x) in C-F show age-grouped monthly incidence estimated from health reports.

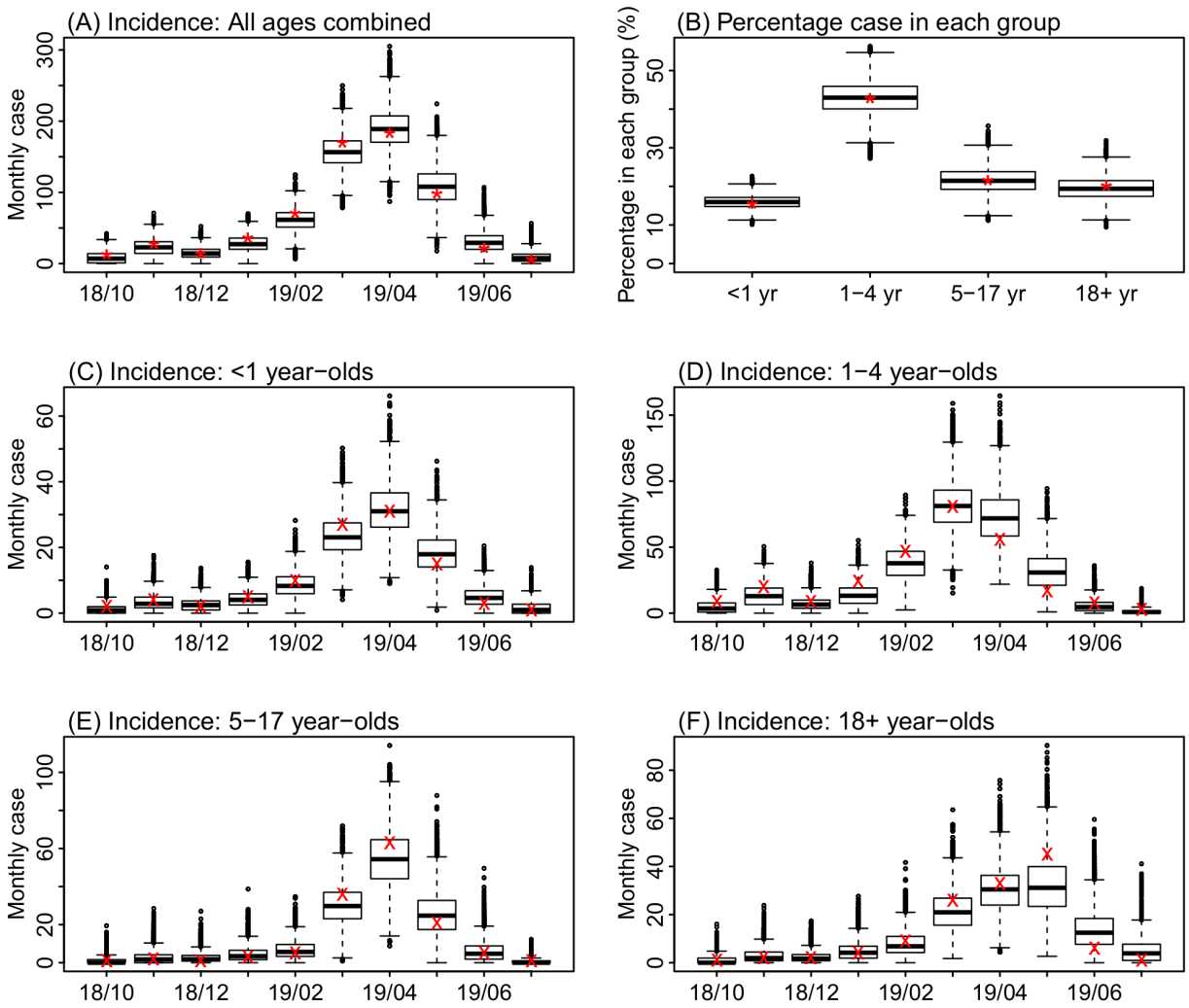

Figure 4. Estimated changes in population susceptibility. Red lines and surrounding areas (y-axis on the left) show the mean and 95% credible intervals of estimates pooled over all 10 model-filter runs (100,000 model realizations in total) for <1 year-olds (A), 1-4 year-olds (B), 5-17 year-olds (C) and 18+ year-olds (D), respectively, at the end of each month from Sep 2018 to July 2019. The initial susceptibilities, estimated at the end of Sep 2018, were computed by adding the total numbers of individuals immunized by the vaccination campaigns in Oct 2018 to the posterior estimates at the end of Oct 2018. For comparison, the grey bars (y-axis on the right) show estimated numbers of individuals immunized during the vaccination campaigns; note that the vaccination campaigns targeted individuals under 19 years and thus is not shown for 18+ year-olds.

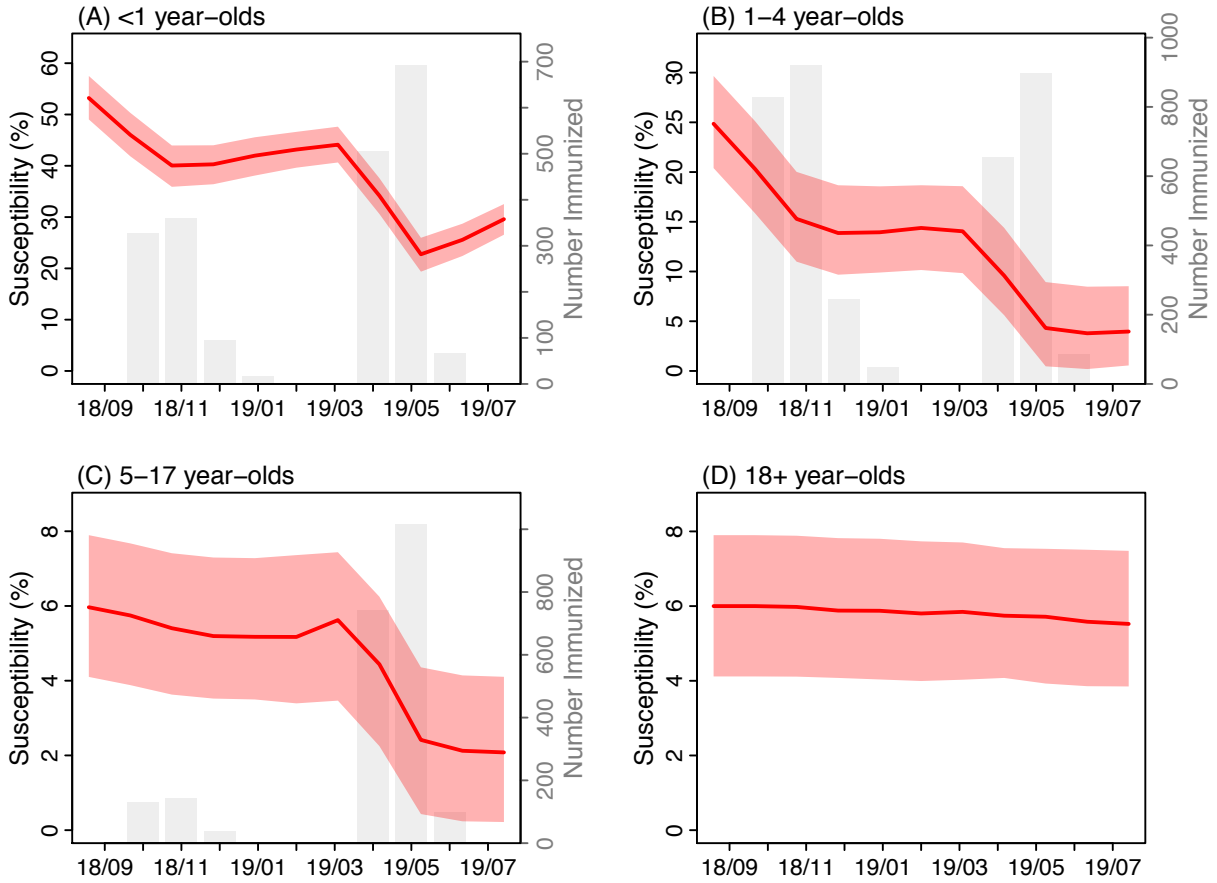

Figure 5. Estimates of key model parameters: (A) the basic reproductive number, (B) the effective reproductive number, (C) infectious period, (D) relative contact rate among 1-4 year-olds, (E) relative contact rate among 5-17 year-olds, and (F) relative contact rate among 18-49 year-olds. Red lines and surrounding areas (y-axis on the left) show the mean and 95% credible intervals of estimates pooled over all 10 model-filter runs (100,000 model realizations in total) made at the end of each month from Oct 2018 to July 2019. For comparison, the grey bars (y-axis on the left) show monthly incidence for all ages (A-C) or the related age groups (D-F).

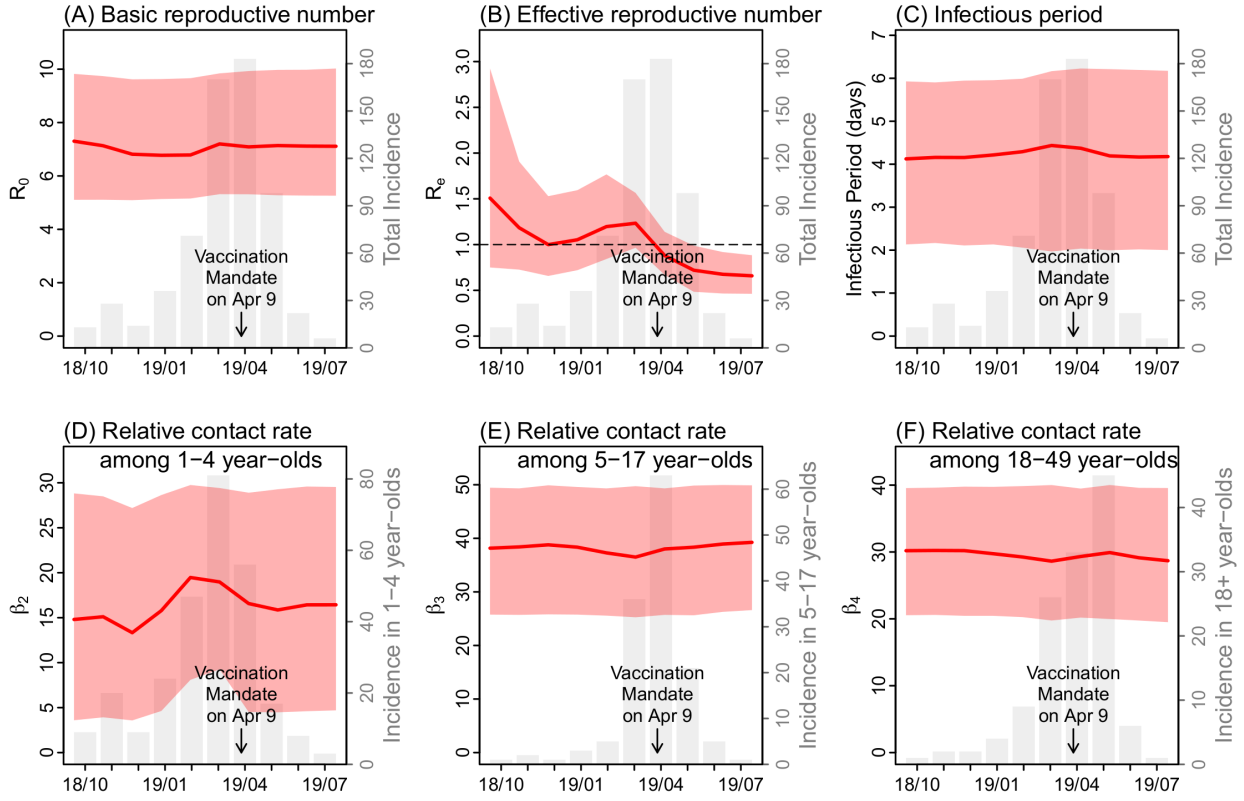

Figure 6. Estimated impact of vaccination campaigns. Box plots show simulated estimates of monthly incidence for all ages (A), percentage of cases reported in each age group (B), and monthly incidence for <1 year-olds (C), 1-4 year-olds (D), 5-17 year-olds (E), and 18+ year-olds (F), should there be no vaccination campaigns. Results are pooled over 10,000 model simulations. Horizontal thick lines show the median of model estimates; box edges show the 25th and 75th percentiles; whiskers show the 2.5th and 97.5th percentiles; and dots show outliers. For comparison, stars (*) in A and B show monthly incidence for all ages and the age distribution, reported as of Aug 6, 2019; crosses (x) in C-F show age-grouped monthly incidence estimated from health reports.

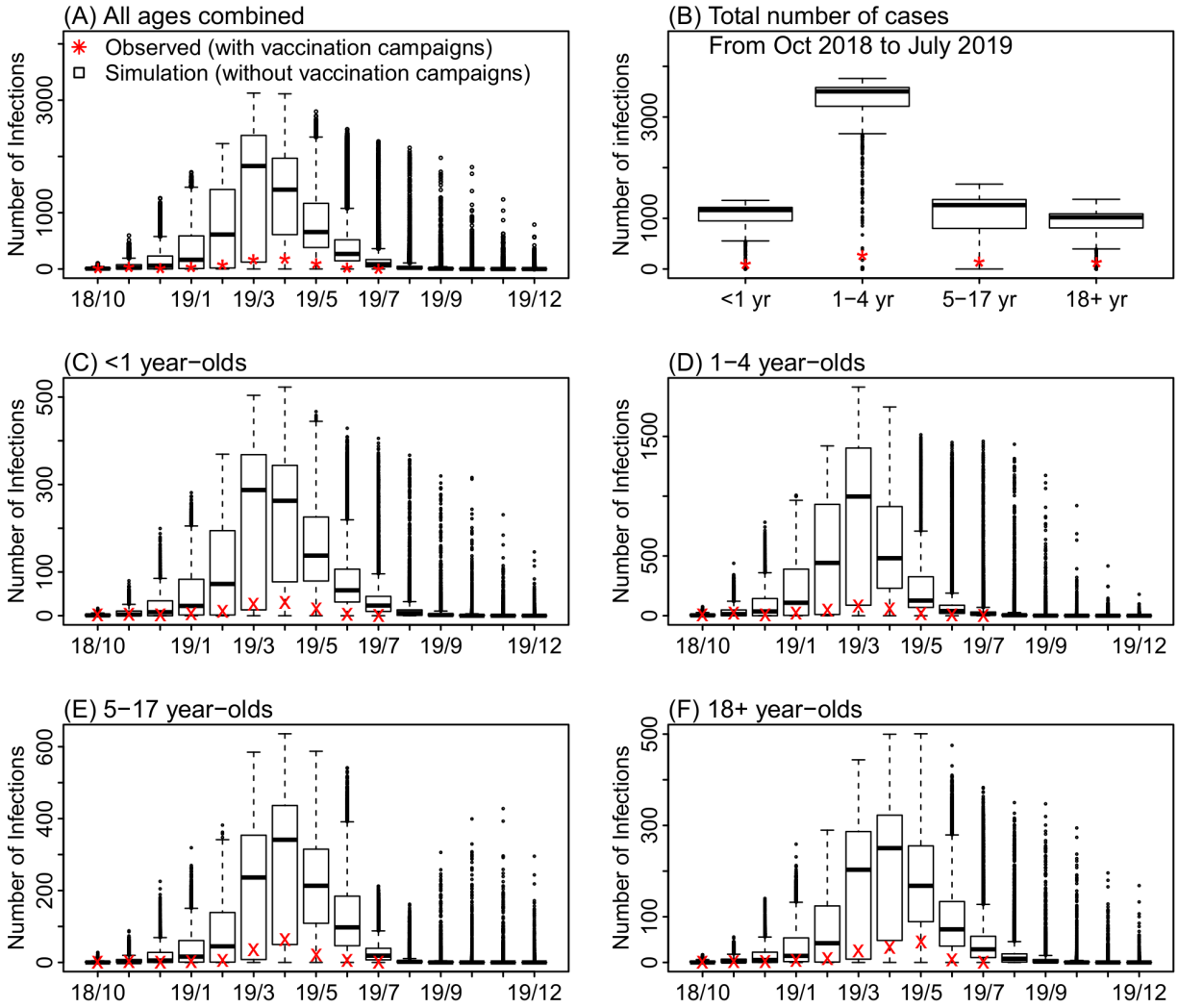

Supplementary Material

Table S1. Comparison of model estimates on initial susceptibility and model performance under different assumptions on vaccination campaigns. The baseline setting is as reported in the main text and alternative settings 1 to 3 are as described in the section "*Sensitivity analysis on vaccination campaigns settings.*" The results are summarized by pooling all 10 model-filter runs (10,000 particles each run and 100,000 model realizations in total). The numbers are the mean and, for the susceptibilities, 95% credible intervals in the parentheses. The initial susceptibilities, estimated at the end of Sep 2018, were computed by adding the total numbers of individuals immunized by the vaccination campaigns in Oct 2018 to the posterior estimates at the end of Oct 2018.

		Model Settings on Vaccination Campaigns			
	Age group	Baseline	Alternative 1	Alternative 2	Alternative 3
Estimated initial susceptibility (%) at end of Sep 2018	<1 year	53.2 (49, 57.5)	54.2 (50, 58.4)	54.2 (50, 58.5)	54.2 (50, 58.5)
	1-4 years	24.9 (20.4, 29.7)	24.9 (20.4, 29.7)	24.9 (20.4, 29.7)	29.9 (25.4, 34.7)
	5-17 years	6.0 (4.1, 7.9)	7.5 (5.1, 9.9)	7.5 (5.1, 9.9)	6.0 (4.1, 7.9)
	18-49 years	6.0 (4.1, 7.9)	7.5 (5.2, 9.9)	7.5 (5.2, 9.9)	7.5 (5.2, 9.9)
	50+ years	6.0 (4.1, 7.9)	6.0 (4.1, 7.9)	6.0 (4.1, 7.9)	6.0 (4.1, 7.9)
Log-likelihood		-255.25	-265.52	-255.25	-257.42
Relative error of total number of cases over the outbreak	<1 year	0.39%	-11.96%	-11.56%	-17.91%
	1-4 years	-0.04%	-7.80%	-6.90%	-8.07%
	5-17 years	-4.13%	14.38%	0.33%	1.84%
	18+ years	-4.70%	7.24%	5.97%	7.95%
	All ages	-1.79%	-0.65%	-3.48%	-4.25%
Root-mean-square-error (RMSE), over Oct 2018 – July 2019	<1 year	1.74	1.86	1.80	2.55
	1-4 years	8.72	8.13	8.17	7.70
	5-17 years	3.91	5.27	3.00	5.10
	18+ years	5.08	4.62	4.30	4.25
	All ages	7.31	7.52	5.88	6.29
Correlation, over Oct 2018 – July 2019	<1 year	0.99	1.00	1.00	0.99
	1-4 years	0.95	0.96	0.96	0.97
	5-17 years	0.99	0.97	0.99	0.97
	18+ years	0.97	0.97	0.97	0.97
	All ages	0.99	0.99	1.00	1.00
1-step-head prediction RMSE, over Oct 2018 – Mar 2019	<1 year	4.37	4.46	4.40	4.60
	1-4 years	17.13	17.34	17.35	25.12
	5-17 years	8.27	8.39	8.37	8.50
	18+ years	4.34	4.93	4.93	5.06
	All ages	27.79	28.23	28.16	35.02
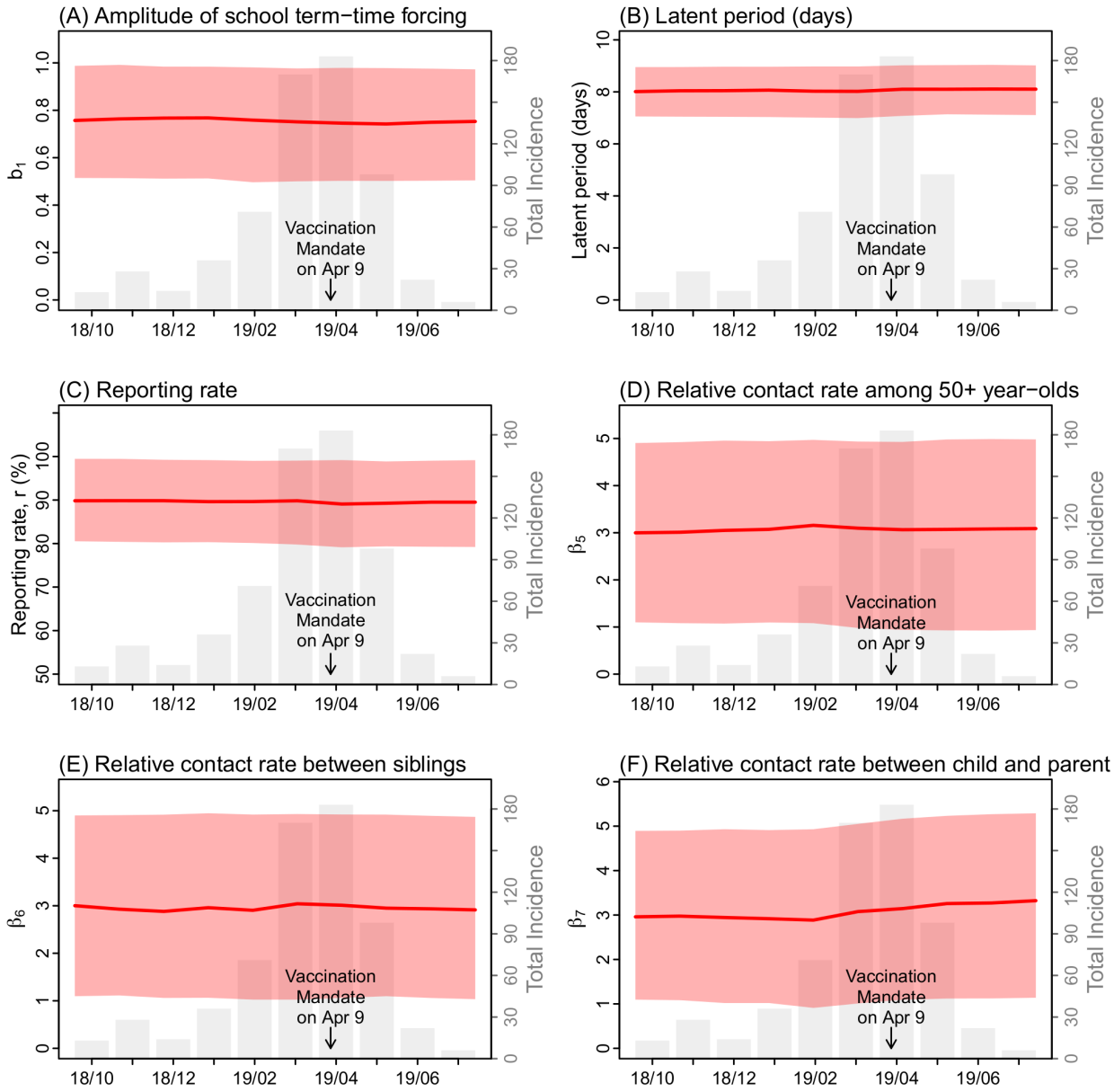
Figure S1. Estimates of model parameters not listed in Figure 5: (A) amplitude of school term-time forcing, (B) latent period, (C) reporting rate, (D) relative contact rate among 50+ year-olds, (E) relative contact rate between 1-4 and 5-17 year-olds (i.e. sibling interactions), and (F) relative contact rate between 18-49 and 1-4 or 5-17 year-olds (i.e. parent-child interactions). Red lines and surrounding areas (y-axis on the left) show the mean and 95% credible intervals of estimates pooled over all 10 model-filter runs (100,000 model realizations in total) made at the end of each month from Oct 2018 to July 2019. For comparison, the grey bars (y-axis on the left) show monthly incidence for all ages. Note that m_1 and m_2 are not shown as both optimal priors are the value 1 (Table 1).